CLASSICAL DESCRIPTION OF MULTIFRAGMENTATION.

D.Cussol

LPC Caen (IN2P3-CNRS/ENSICAEN et Université), F-14050 Caen Cedex , France

Abstract

Results on multifragmentation from Classical N Body Dynamics calculations are shown. It will be shown that the signals of a phase transition (negative heat capacity, Fisher's scaling, bimodality) and the hierarchy and alignment effects may be described in a unique framework. Qualitative comparisons to experimental data are made and the significance of these observations is discussed.

1. INTRODUCTION

Describing the multifragmentation of nuclei is still a challenge. The full understanding of this process is not yet achieved. Many questions are open. Is multifragmentation a thermalised process? If not, what is the meaning of the thermal description of this process? What is the influence of the entrance channel? How can we deduce the equation of state of infinite nuclear matter from this process? Many models have been built to describe the experimental observations. Among these models are the classical molecular dynamics simulations [1, 2, 3, 4, 5, 6]. The main advantages of these models is their simplicity and that no approximations are necessary. The main drawback is that quantum mechanics effects are not present. We will present here the results of one of these codes: Classical N-Body Dynamics (labelled CNBD in the following). This code only contains a four parameter polynomial two-body interaction without any Coulomb-like interaction nor quantum corrections. A complete description of this code is made in [7]. CNBD is used here to check to which extent this simple simulation is qualitatively similar or not to the data and to determine what kind of information we can extract from it. The units used in CNBD are arbitrary and called Simulation Units (labeled S.U.). Energies will be in Energy Simulation Units (E.S.U.), distances in Distance Simulation Units (D.S.U.) and times in Time Simulation Units (T.S.U.).

The clusters are defined in the following way: two particles belong to the same cluster if their relative distance is smaller than or equal to the range of the interaction. The intermediate mass fragments (labelled IMF) are the clusters which contain at least three particles ($N \geq 3$). The fragments are identified at a time greater than the "freeze-out" time after which the clusters do not interact anymore amongst themselves.

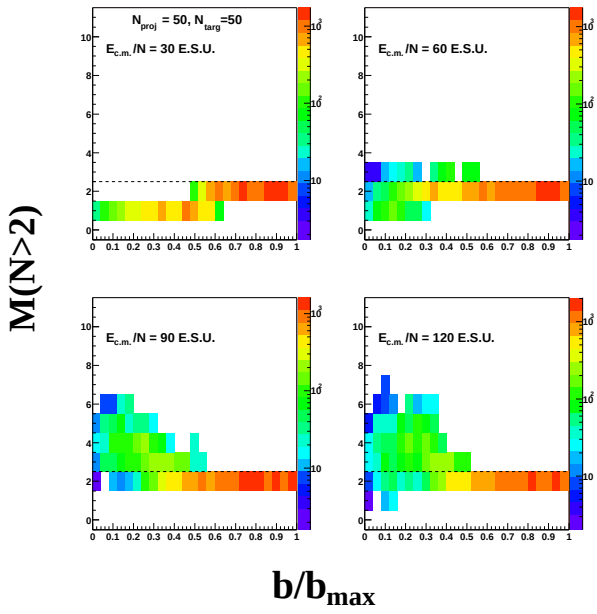

Figure 1: Correlation of the fragment multiplicity with the reduced impact parameter for a 50 particle projectile colliding with a 50 particle target at four $E_{c.m.}$/N values.

Let us first identify in which initial conditions the multifragmentation process occurs. On figure 1 is presented the correlation between the fragment multipliciy (clusters with at least three particles) and the reduced impact parameter $b_{red} = b/b_{max}$, at four arbitrarily chosen available en-

ergies per particle in the centre of mass frame $E_{c.m.}$/N. The link between these energies and the static properties of the classical cluster will be made in the last section. The multifragmentation process will be identified as the process which produces at least three fragments. One can see that multifragmentation starts to occur at $E_{c.m.}$/N=60 E.S.U. for reduced impact parameters roughly below 0.5. At a lower energy, only fusion process and binary collisions are seen. At higher energies, the multiplicity of fragments is higher but multifragmentation occurs only for collisions with $b_{red} \leq 0.5$. At higher impact parameters, only binary collisions are observed.

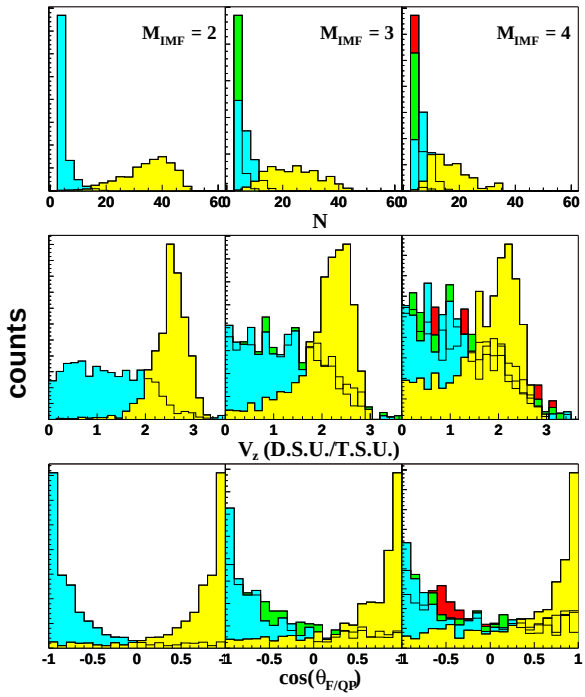

Figure 2: Size (uppermost row), parallel velocity (middle row) and cos($\theta_{F/QP}$)(lower row) distributions for the 50+50 system at $E_{c.m.}$/N=120 E.S.U. (see the definitions of the angle in [8]). The columns correspond to different fragment mutiplicities (from M_{IMF}=2 to M_{IMF}=4 from left to right). The shading of the distribution is darker and darker according to the rank of the fragment in the event (the lightest shading corresponds to the heaviest fragment in the event).

2. PERIPHERAL AND SEMI-PERIPHERAL COLLISIONS

One can first study the global properties of multifragmentation for the major part of the cross section. Let us first check in this section if the hierarchy effect seen in nucleus-nucleus collisions [8] is present in this simple simulation. Figure 2 shows the size distribution, the velocity distribution and the angular distribution (see the definition of cos($\theta_{F/QP}$) in [8]) of the fragments according to the fragment multiplicity (columns) and to the ranking in size of the fragment in the event. This figure is very similar to the one obtained for experimental data [8]: the heaviest fragment is on average the fastest and its emission direction is very close to the recoil velocity direction of the recontructed quasi-projectile (cos($\theta_{F/QP}$) distribution of the heaviest fragment peaked at 1). The same similarity is obtained on angular distributions (see the definition of θ_{prox} in [8]) as shown in figure 3: the angular distributions of the most symmetrical break-up (first row) are almost flat whereas the angular distributions of the most asymmetrical break-ups are strongly for-

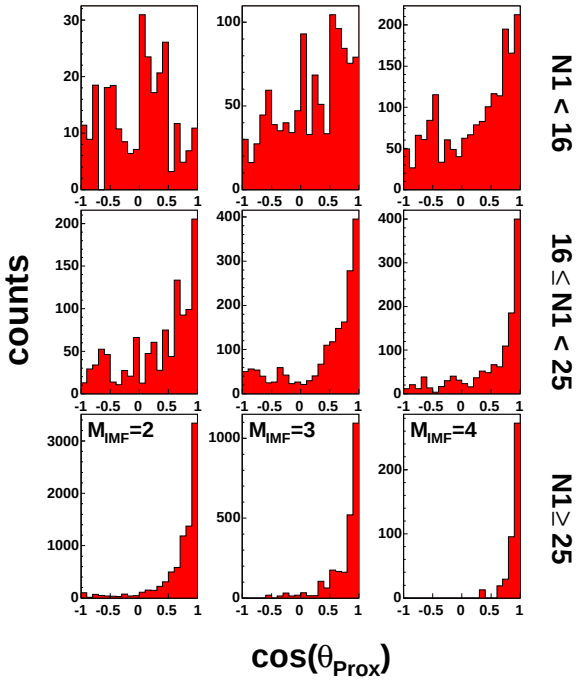

Figure 3: $cos(\theta_{prox})$ distributions for the 50+50 system at $E_{c.m.}$/N=120 E.S.U.. The columns correspond to the different fragment multiplicities from 2 to 4. The rows correspond to different ranges for the size N_1 of the heaviest fragment: the most symmetrical break-ups (low N_1 values) correspond to the uppermost row and the most asymmetrical break-ups (high N_1 values) correspond to the lower row.

ward peaked, regardless of the fragment multiplicity.

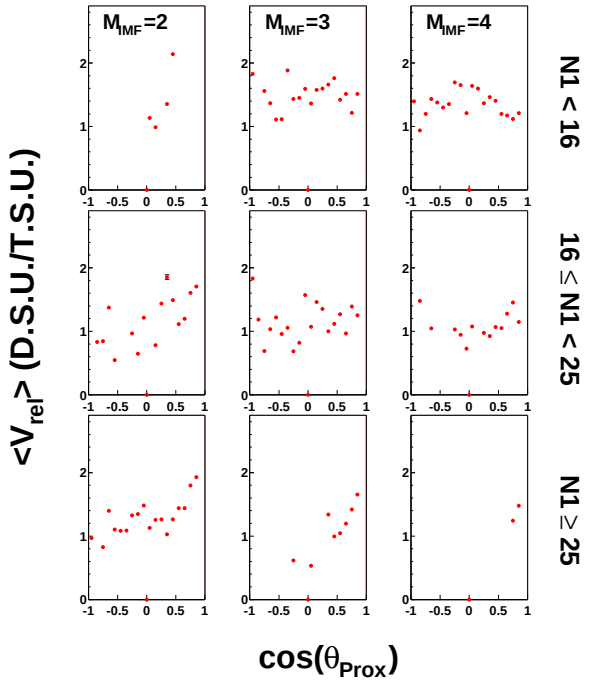

Figure 4: Evolutions of the average relative velocity v_{rel} with $cos(\theta_{prox})$ for the 50+50 system at $E_{c.m.}$/N=120 E.S.U..

The same qualitative agreement is even obtained on the correlation between the relative velocity of the heaviest fragment and the other fragments and the break-up direction (see [8] for the definitions of v_{rel} and θ_{prox}). For the the most symetrical break-ups (first row), almost no variation of v_{rel} with $cos(\theta_{prox})$ is seen whereas a clear increase of v_{rel} with $cos(\theta_{prox})$ is seen for the most symmetrical break-ups (last row).

The properties of multifragmentation in this classical simulation are qualitatively very similar to those observed in nucleus-nucleus collisions. For this simulation, multifragmentation results from the formation and the fast break-up of a neck between the quasi-projectile and the quasi-target. Providing that these conclusions made for the classical simulation can be extended to the nucleus-nucleus collisions, this would support the conclusion drawn in [8]. One has also to notice that this overall qualitative agreement has been obtained without adding or modifying any parameters, whereas such additional effective parameters are needed in statistical descriptions [9].

3. CENTRAL COLLISIONS

In the previous section an overall qualitative agreement of the simulation with experimental data was obained for the major part of the cross section. For the most central collisions ($b_{red} < 0.1$), signals of phase transition have been observed in exerimental data. In this section, we will check the existence in the simulation of only three of these signals.

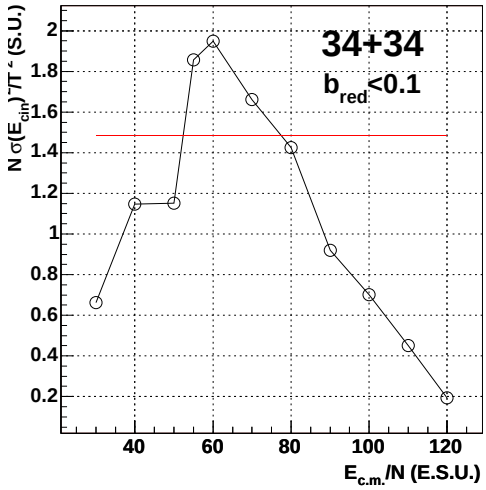

Figure 5: Variations of the reduced fluctuations $\sigma(E_{kin})/T^2$ with $E_{c.m.}$/N for the central collisions of the 34+34 system. The thick horizontal line corresponds to the expected canonical value of the heat capacity C_{kin} for the kinetic energy.

Let us start with the negative heat capacity [10, 11, 12]. In the case of a phase transition, abnormal fluctuations should be seen. More precisely, the reduced fluctuations of the kinetic energy $\sigma(E_{kin})/T^2$ should be greater than the heat capacity for the kinetic energy $C_{kin} \approx \frac{3}{2}$. The variations of $\sigma(E_{kin})/T^2$ with $E_{c.m.}$/N for central collisions ($b_{red}< 0.1$) of a 34 particle cluster colliding a 34 particles target are shown on figure 5. Such abnormal fluctuations are seen for $E_{c.m.}$/N ranging from $\approx 55 E.S.U.$ to $\approx 85 E.S.U.$, indication that a phase transition may occur in the classical simulation.

The second signal which will be studied has been proposed by the Berkeley team [13, 14]. In the case of a phase transition, the fragment production rate n_N can be parametrised by using the Fisher liquid drop formula when the system

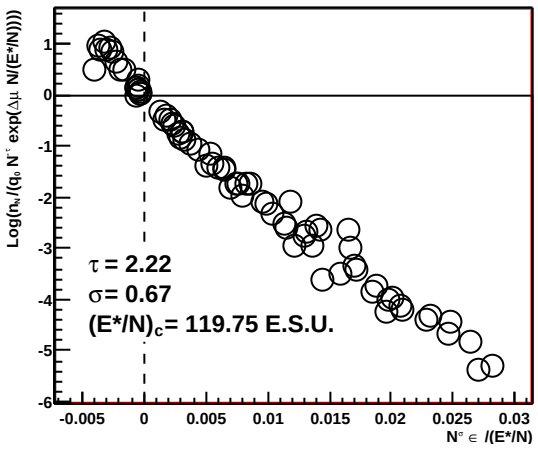

Figure 6: Rescaled production rates by using the Fisher's formula for the 50+50 central ($b_{red}< 0.1$) collisions and for $E_{c.m.}$/N ranging from 30 E.S.U. to 120 E.S.U..

is close to the critical point. With the appropriate scaling, all the production rates should collapse on a single straight line. When applying this scaling for the central collisions ($b_{red}< 0.1$) of a 50 particule projectile colliding with a 50 particle target, all the production rates collapse on a single straight line (figure 6), indicating also that a phase transition may occur in this classical simulation. The values of the critical parameters $\sigma = 0.67$ and $\tau = 2.22$ are also very close to the values obtained in nucleus-nucleus collisions and close to the expected values for a Van der Waals fluid. The meaning of the value obtained for the critical energy is not clear.

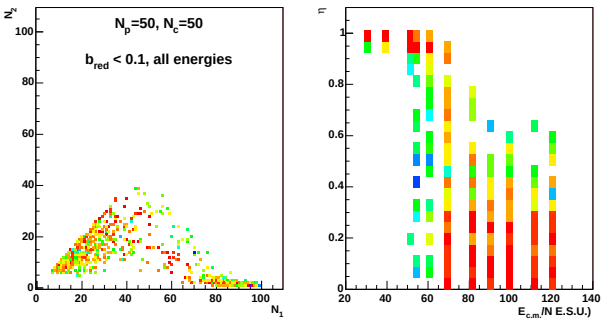

Figure 7: Bimodality plots for central 50+50 collisions. Left panel: correlation of the size of the size N_1 of the heaviest fragment and the size N_2 of the second heaviest fragments. Right panel: correlation of the asymmetry η of the break-up and $E_{c.m.}$/N.

The last signal we will check in this section is the bimodality. In the case of a phase transition, the distribution of an order parameter of the transition should exhibit two bumps in the coexistence region [15, 16]. Experimentally, it has been found that the size of the heaviest cluster, or the asymmetry $\eta = \frac{N_1-N_2}{N_1+N_2}$ of the break-up is an order parameter of the transition [17, 18]. When plotting the correlation of the size N_1 of the heaviest fragment and the size N_2 of the second heaviest fragment (left panel in figure 7), one sees clearly two populated areas: one with a big frament and a small one ("liquid phase") and a second one with two fragments with almost the same size ("gas phase"). When looking at the evolution of η with $E_{c.m.}$/N (figure 7, right panel), the jump from one configuration to the other is very abrupt, the "coexistence" zone being quite sharp and centred around $E_{c.m.}/\mathrm{N} \approx 60 E.S.U.$. Here again the qualitative similarity with the experimental data is quite surprising.

We have seen in this section that as in experimental data, the classical simulation exhibits at the same time different signals of a phase transition. The energy of the transition is around $E_{c.m.}/\mathrm{N} \approx 60\ E.S.U.$ which is also the threshold energy for multifragmentation to occur. But what is the nature of the transition? Is the system thermalised during this transition?

4. DISCUSSIONS

It has been shown in a previous work that indeed the thermal energy per particle that a classical cluster can sustain does not exceed the potential energy of the least bound particle of this cluster [19]. This energy is very sensitive to the surface properties of the clusters. For the system sizes which have been shown here, this energy $E_{leastbound}$ is around 60 E.S.U, which is the threshold energy for multifragmentation and the energy found for the different signals studied in the previous section. It has also been shown in reference [19] that the fragment production for central collisions occurs in an incompletely thermalised situation. Indeed, above $E_{c.m.}/\mathrm{N} \approx 60\ E.S.U.$, the additionnal energy is stored not as thermal energy in clusters but rather as expansion energy. As in the data [20] the appearance of expansion energy and the occurence of multifragmentation are extremely linked. It is also

worth noticing that the binding energy per particle E_{bind}/N (bulk property) plays a minor role in multifragmentation compared to $E_{leastbound}$ (surface property).

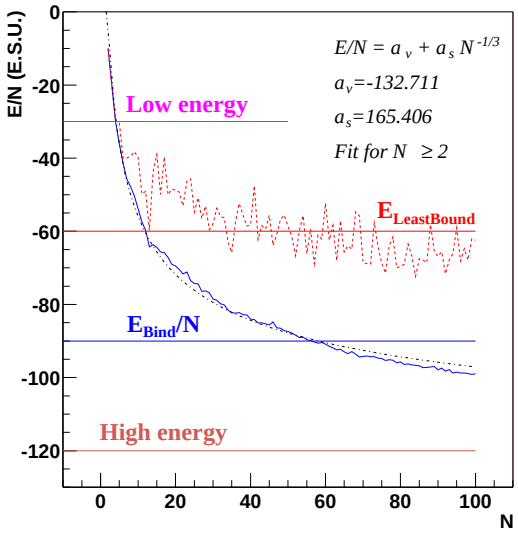

Figure 8: Binding energy per particle (full line) and potential energy of the least bound particle (dashed line) as a function of the number N of particles in the cluster. The four horizontal lines correspond to the four energies shown in figure 1.

From these observations, we can try to link the behaviour of the classical colliding systems to their properties as shown in figure 8. At $E_{c.m.}$/N=30 E.S.U., the collision leads to the fusion/evaporation process for central collisions and for binary collisions (mass transfers, particle exchange, deeply inelastic collisions) for peripheral reactions. This energy can be identified as a "low energy". At $E_{c.m.}/N = 60\ E.S.U.$, which is close to $E_{leastbound}$, multifragmentation takes place and signals of phase transition are present for the most central collisions. A neck formation and its fast break-up is the dominant process for semi-central collisions. This energy can be identified as an "intermediate energy". At $E_{c.m.}/N = 90\ E.S.U.$, which is close to E_{bind}/N , the system is already in a "high energy" regime: multifragmentation is dominant for central collisions, the size of the fragments being smaller and smaller with increasing energy; binary collisions and participant/spectator processes occur for the peripheral collisions. It could be worth studying if this picture can apply to nuclear systems.

Since in CNBD $E_{leastbound}$ is the key energy for the multifragmentation process and is an upper limit for the validity of thermal descriptions of the process, it seems at least questionable to use the multifragmentation process to reconstruct the equation of state of infinite matter. Indeed, the whole phase diagram is not accessible in collisions since the thermal energy is limited well below the binding energy of the clusters. If this can apply to nuclear systems, the search for the equation of state of infinite nuclear matter from nucleus-nucleus collisions should be reconsidered. This would also raise the question of the real meaning of the thermal descriptions commonly used in our community. This question can be addressed in CNBD by comparing the behaviours of thermalised and colliding systems with the same size and the same total energy.

5. CONCLUSIONS

We have shown that a good qualitative agreement of the CNBD simulation with experimental data is observed. Such an agreement was not expected since many ingredients are missing in the simulation (Coulomb interaction, quantum mechanics). These qualitative similarities are obtained in a unique framework without adding or modifying parameters. The reasons for such an agreement are not clear, but it may mean that the N-body effects (conservation laws, N-body correlations) are dominant in both cases.

For multifragmentation, the "hierarchy effect" and the internal correlations are obtained for semi-peripheral reactions and signals of phase transitions are seen for central collisions. The meaning of such signals in CNBD is not clear since multifragmentation in the simulation is not a thermalised process. In all cases, the energy of the least bound particle is the key energy for understanding the multifragmentation of classical systems.

The questions of the meaning of the thermal descriptions and the possibility to reconstruct the equation of state of infinite matter from the collisions have now to be adressed. This classical simulation is an effective and powerful tool to give a part of the answer.

6. REFERENCES

[1] T.J.Schlagel and V.R.Pandharipande, Phys. Rev. **C36** (1987) 162.

[2] C.Dorso and J.Randrup, Phys. Lett. **B215** (1988) 611.

[3] V.Latora *et al.*, Nucl. Phys. **A572** (1994) 477.

[4] J.Bondorf *et al.*, Nucl. Phys. **A624** (1997) 706.

[5] X.Campi, H.Krivine and N.Sator, Nucl. Phys. **A681** (2000).

[6] A.Strachan and C.Dorso, Phys. Rev. **C59** (1999) 285.

[7] D.Cussol, Phys. Rev. **C65** (2002) 054614.

[8] J.Colin *et al.* (INDRA Collaboration), Phys. Rev. **67** (2003) 064603.

[9] J.Normand, Ph. d. thesis, Université de Caen (2001).

[10] F.Gulminelli and Ph.Chomaz, Phys. Rev. Lett. **82** (1999) 1402.

[11] M.D'Agostino *et al.*, Phys. Lett. **473** (2000) 219.

[12] M.D'Agostino *et al.*, Nucl. Phys. **A699** (2002) 795.

[13] J.B.Elliott *et al.*, Phys. Rev. Lett. **88** (2002) 042701.

[14] J.B.Elliott *et al.*, Phys. Rev. **C67** (2003) 024609.

[15] Ph.Chomaz and F.Gulminelli, http://arxiv.org/abs/cond-mat/0210456 (2003).

[16] B.Tamain *et al.* (INDRA Collaboration), IWM2003 (2003).

[17] R.Botet *et al.*, Phys. Rev. Lett. **86** (2001) 3514.

[18] J.D.Frankland *et al.* (INDRA Collaboration), IWM2003 (2003).

[19] D.Cussol, Phys. Rev. **C68** (2003) 014602.

[20] F.Rami *et al.*, IWM2003 (2003).